Anesthesiology
2000; 92:1757-68

Isoflurane Alters the Recirculatory Pharmacokinetics of Physiologic Markers

Michael J. Avram, Ph.D., Tom C. Krejcie, M.D.,* Claus U. Niemann, M.D.,† Cheri Enders-Klein, B.A.,‡ Colin A. Shanks, M.D.,§ Thomas K. Henthorn, M.D.‖*

Background: **Earlier studies have demonstrated that physiologic marker blood concentrations in the first minutes after administration, when intravenous anesthetics exert their maximum effect, are determined by both cardiac output and its distribution. Given the reported vasodilating properties of isoflurane, we studied the effects of isoflurane anesthesia on marker disposition as another paradigm of altered cardiac output and regional blood flow distribution.**

Methods: **The dispositions of markers of intravascular space and blood flow (indocyanine green), extracellular space and free water diffusion (inulin), and total body water and tissue perfusion (antipyrine) were determined in four purpose-bred coonhounds. The dogs were studied while awake and while anesthetized with 1.7%, 2.6%, and 3.5% isoflurane (1.15, 1.7, and 2.3 minimum alveolar concentration, respectively) in a randomized order determined by a Latin square experimental design. Marker dispositions were described by recirculatory pharmacokinetic models based on very frequent early, and less frequent later, arterial blood samples. These models characterize the role of cardiac output and regional blood flow distribution on drug disposition.**

Results: **Isoflurane caused a significant and dose-dependent decrease in cardiac output. Antipyrine disposition was profoundly affected by isoflurane anesthesia, during which nondistributive blood flow was maintained despite decreases in cardiac output, and the balance between fast and slow tissue volumes and blood flows was altered.**

Conclusions: **The isoflurane-induced changes in marker disposition were different than those the authors reported previously for halothane anesthesia, volume loading, or hypovolemia. These data provide further evidence that not only cardiac output but also its peripheral distribution affect early drug concentration history after rapid intravenous administration. (Key words: Blood flow; cardiac output; physiologic models.)**

EARLY drug distribution (*i.e.*, front-end kinetics) determines the blood drug concentration *versus* time relationship during the time when rapidly administered intravenous anesthetics produce their maximum effect.[1] Early blood drug concentration history is affected by both cardiac output (CO) and drug recirculation.

Although the importance of CO in determining anesthetic induction dose may seem intuitive to anesthesiologists today, it was first formally recognized by Price[2] in 1960 and has only recently received renewed attention. The tissue distribution of alfentanil in humans was demonstrated to be largely dependent on CO.[3] The thiopental dose required to reach electroencephalogram burst suppression in humans was dependent on CO,[4] as were peak concentrations of rapidly infused hypnotics in computer simulations of drug administration[5] and studies in sheep.[6,7] CO has also been identified as a critical covariate in predicting fentanyl pharmacokinetic changes that occur with hemorrhagic shock.[8]

The effect of recirculation on early drug concentrations is best understood by considering what we have called "nondistributive blood flow."[9,10] Nondistributive blood flow is that portion of CO that does not expose drug to tissue uptake (*i.e.*, intercompartmental clearances to peripheral tissue compartments) or to elimination from the body (elimination clearance). Thus, nondistributive blood flow returns (shunts) drug to the central circulation after minimal tissue equilibration.

An index of drug exposure of the sites of drug action, such as the brain, is the area under the blood drug

* Associate Professor.

† Research Fellow. Current position: Resident in Anesthesia, Department of Anesthesia and Perioperative Care, University of California at San Francisco, San Francisco, California.

‡ Research Technician. Current position: Graduate Student, College of Pharmacy, University of Illinois at Chicago, Chicago, Illinois.

§ Professor (Deceased.)

‖ Associate Professor. Current position: Associate Professor and Chairman, Department of Anesthesiology, University of Colorado Health Sciences Center, Denver, Colorado.

Received from the Department of Anesthesiology, Northwestern University Medical School, Chicago, Illinois. Submitted for publication September 13, 1999. Accepted for publication February 4, 2000. Supported in part by grants no. GM43776 and GM47502 from the National Institutes of Health, Bethesda, Maryland. Presented in part at the annual meeting of the American Society of Anesthesiologists, Orlando, Florida, October 18-21, 1998.

Address reprint requests to Dr. Avram: Northwestern University Medical School, Department of Anesthesiology, 303 E. Chicago Avenue, CH-W139, Chicago, Illinois 60611-3008. Address electronic mail to: mja190@nwu.edu

concentration *versus* time curve ($AUC_{0\text{-}n\ min}$).[11] The time (n min) over which $AUC_{0\text{-}n\ min}$ should be calculated is that time during which blood concentrations are above an effective threshold for a given drug. For drugs used in anesthesia, this time is the first few minutes after rapid intravenous administration. The $AUC_{0\text{-}n\ min}$ in the first minutes after rapid intravenous drug administration can be broken down into two components.[12] The first component is the AUC calculated for the initial arterial drug concentrations resulting from the passage of drug from the site of injection through the heart and lungs of the central circulation and extrapolated to infinity from the slope of the downward limb before recirculation. This first-pass AUC ($AUC_{first\text{-}pass}$) is determined by drug dose and CO, assuming no drug uptake by pulmonary tissue (*i.e.*, $AUC_{first\text{-}pass}$ = dose/CO). The second component is determined by the amount of drug returning to the central circulation after loss from the blood due to uptake by peripheral tissues and elimination from the body. The resultant arterial concentrations are thus due to recirculation (AUC_{recirc}) and give rise to a recirculatory peak.[10] The sum of $AUC_{first\text{-}pass}$ and AUC_{recirc} thus results in the $AUC_{0\text{-}n\ min}$, or active-site drug exposure over the time frame of interest. A recirculatory pharmacokinetic model is able to resolve these two components and thereby characterize the mechanism(s) responsible for interindividual differences in drug reactivity.

We have developed such a recirculatory multicompartmental pharmacokinetic model of drug disposition based on very frequent early arterial blood samples.[10] This model describes the simultaneous disposition of physiologic markers, serving as pharmacokinetic surrogates for drugs, that mix within the intravascular space from which they distribute to interstitial fluid space and total body water by blood flow and free water diffusion.[13] The recirculatory model incorporates physiologic factors, such as CO and its distribution (*i.e.*, regional blood flows), in a description of drug disposition. The model estimates blood flow to tissue compartments based on the calculated intercompartmental clearances of a flow-limited tissue distribution marker (*i.e.*, intercompartmental clearance equals tissue blood flow in the absence of diffusion barriers). The model uses blood marker concentrations of the recirculatory peak to describe nondistributive blood flow that, because of arteriovenous anastomoses or significant diffusion barriers, returns blood to the central circulation after minimal marker loss due to tissue uptake or elimination.

Applying this model, we have described previously the distribution of physiologic markers in dogs under different levels of halothane anesthesia[14] and in volume-loaded as well as mildly and moderately hypovolemic dogs.[12] These studies have demonstrated that not only CO but also regional blood flow, including, specifically, that fraction of CO represented by nondistributive blood flow, affect early drug concentration history after rapid intravenous administration. These studies have also demonstrated that the relative impact of CO and regional blood flow vary, depending on the characteristics of the marker being studied and the physiologic circumstances of the subject.

Because of the reported vasodilating properties of isoflurane,[15] the purpose of the present study was to determine the effects of different levels of isoflurane anesthesia on physiologic marker distribution by mixing, flow, and diffusion in dogs as another paradigm of altered CO and regional blood flow.

Materials and Methods

Experimental Protocol

The design of this pharmacokinetic study entailed 16 individual experiments. Four purpose-bred male coonhounds, weighing 24–37 kg (28.4 ± 5.9 kg; see table 1), were studied on four occasions each in this Institutional Animal Care and Use Committee–approved study. Approximately 1 month before being studied, a Vascular-Access-Port (Access Technologies, Skokie, IL) was implanted with its catheter tip positioned near the aortic bifurcation *via* a femoral artery of each dog to facilitate frequent percutaneous arterial blood sampling.[16]

All dogs were studied while awake (0% isoflurane, control) and while anesthetized with isoflurane at end-tidal concentrations of 1.7%, 2.6%, and 3.5%, which correspond to 1.15, 1.7, and 2.3 minimum alveolar concentration.[17,18] The order in which these studies were conducted in each dog was randomized using a Latin square experimental design. The details of the preparation and conduct of the individual studies have been described in detail previously.[14]

In the isoflurane studies, anesthesia was induced with methohexital (10–15 mg/kg intravenously), the trachea was intubated, and the animal was placed in the left lateral decubitus position. Mechanical ventilation was instituted to control end-tidal carbon dioxide tension at 30 ± 5 mmHg. Anesthesia was maintained with 1.7%, 2.6%, or 3.5% isoflurane in oxygen, and end-tidal concentrations were monitored with a side-stream infrared analyzer.

A flow-directed thermal dilution pulmonary artery catheter was inserted through a right external jugular vein sheath introducer in both awake and anesthetized dogs. The pulmonary artery catheter was subsequently used to determine thermal dilution CO as well as to facilitate right atrial administration of the physiologic markers.

The study was not begun until the dog was hemodynamically stable (approximately 1 h) after the targeted end-tidal isoflurane concentration had been reached. This was defined as less than 10% variation of CO and pulmonary and systemic arterial blood pressures over a 30-min period when heart rate and blood pressures were measured continuously and CO was determined at least every 15 min.

Indocyanine green (ICG; Cardio-Green; Hynson, Westcott, and Dunning, Baltimore, MD), 5 mg in 1 ml of ICG diluent, [^{14}C]-inulin (DuPont NEN, Boston, MA), 30 μCi in 1.5 ml of ICG diluent, and antipyrine (Sigma, St. Louis, MO), 25 mg in 1 ml of ICG diluent, were placed sequentially in a 76-cm-long intravenous tubing (4.25 ml priming volume) and connected to the proximal injection port of the pulmonary artery catheter. At the onset of the study (time t = 0 min), the markers were flushed into the right atrium within 4 s using 10 ml of 5% dextrose in water, allowing the simultaneous determination of dye and thermal dilution COs. Arterial blood samples were collected *via* the Vascular-Access-Port every 0.03 min for the first 0.48 min and every 0.06 min for the next 0.54 min using a computer-controlled roller pump (Masterflex; Cole-Parmer, Chicago, IL). Subsequently, 35 3-ml arterial blood samples were drawn manually at 0.2-min intervals to 2 min, at 0.5-min intervals to 4 min, at 5 and 6 min, every 2 min to 20 min, at 25 and 30 min, every 10 min to 60 min, every 15 min to 120 min, and every 30 min to 360 min.

Analytical Methods

Plasma ICG concentrations of all samples obtained up to 20 min were measured on the study day by the high-performance liquid chromatography technique of Grasela *et al.*[19] as modified in our laboratory.[10] Plasma [^{14}C]-inulin concentrations of all samples were determined by liquid scintillation counting, using an external standard method for quench correction.[20] Plasma antipyrine concentrations were measured in all samples using a modification of a high-performance liquid chromatography technique developed in our laboratory.[10,21]

To interpret antipyrine intercompartmental clearances in relation to blood flow, the recirculatory models were constructed on the basis of whole blood marker concentrations. Plasma ICG and inulin concentrations were converted to blood concentrations by multiplying them by one minus the hematocrit, as neither ICG nor inulin partitions into erythrocytes. Plasma antipyrine concentrations were converted to blood concentrations using an *in vivo* technique that corrects for antipyrine partitioning into erythrocytes by calculating its apparent dose assuming an erythrocyte:plasma partition coefficient of one; the product of CO and $AUC_{first\text{-}pass}$ for the plasma antipyrine concentration *versus* time curve equals dose when its erythrocyte:plasma partitioning is one.[10,22]

Pharmacokinetic Model

The pharmacokinetic modeling methodology (fig. 1) has been described in detail previously.[10,14] It is based on the approach described by Jacquez for obtaining information from outflow concentration histories, the so-called inverse problem.[23] Inulin and antipyrine distributions were analyzed as the convolution of their intravascular behavior, determined by the pharmacokinetics of concomitantly administered ICG, and tissue distribution kinetics.[10]

Arterial ICG, inulin, and antipyrine concentration *versus* time data before evidence of recirculation (*i.e.*, first-pass data) were weighted uniformly and fit to the sum of two Erlang distribution functions using TableCurve2D (ver 3.0; Jandel Scientific, San Rafael, CA) on a Pentium-based personal computer (Gateway 2000, North Sioux City, SD); two parallel, lumped pathways with different transit characteristics reflect the heterogeneity in the distribution of transit times in the pulmonary circulation.[22] Because neither ICG nor inulin distribute beyond the intravascular space before recirculation, they were modeled simultaneously to improve the confidence in the model parameters of the central (first-pass) circulation. Antipyrine has measurable pulmonary tissue distribution during this time and was modeled independently; the antipyrine pulmonary tissue volume ($V_{T\text{-}P}$) is the difference between the antipyrine central volume ($MTT_{antipyrine} \cdot CO$) and the central intravascular volume codetermined by ICG and inulin ($MTT_{ICG,inulin} \cdot CO$).

In subsequent pharmacokinetic analysis, these descriptions of the central circulation were incorporated as parallel linear chains, or delay elements, into independent recirculatory models for the individual markers using SAAM II (SAAM Institute, Seattle, WA) implemented on a Pentium-based personal computer.[22,24] The concentration–time data were weighted, assuming a proportional variance model, in proportion to the inverse of

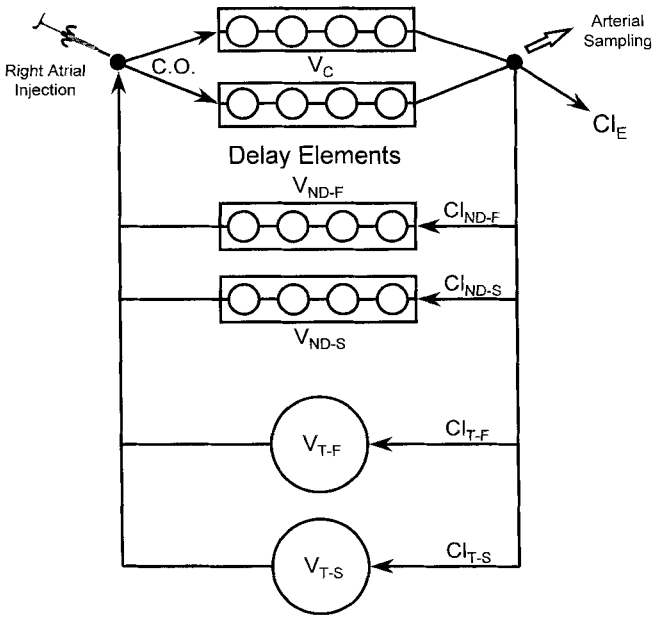

Fig. 1. The general model for the recirculatory pharmacokinetics of indocyanine green (ICG), inulin, and antipyrine. The central circulation of all three markers, defined by the central delay elements (V_C), receives all of cardiac output (CO). The delay elements are represented generically by rectangles surrounding four compartments, although the actual number of compartments needed varied between 2 and 30 in any given delay. Beyond the central circulation, the CO distributes to numerous circulatory and tissue pathways that lump, on the basis of their blood volume to blood flow ratios or tissue volume to distribution clearance ratios (MTTs), into fast (Cl_{ND-F}, V_{ND-F}) and slow (Cl_{ND-S}, V_{ND-S}) peripheral-blood circuits (ICG) or nondistributive peripheral pathways (inulin and antipyrine) and fast (Cl_{T-F}, V_{T-F}) and slow (Cl_{T-S}, V_{T-S}) tissue volume groups. ICG, which distributes only within the intravascular space, does not have fast and slow tissue volumes. Antipyrine does not have an identifiable second nondistributive peripheral circuit. The elimination clearance (Cl_E) of all three markers are modeled from the arterial sampling site without being associated with any particular peripheral circuit.

the square of the observed value. Possible systematic deviations of the observed data from the calculated values were sought[25] using the one-tailed one-sample runs test,[26] with $P < 0.05$, corrected for multiple applications of the runs test, as the criterion for rejection of the null hypothesis. Possible model misspecification was sought by visual inspection of the measured and predicted marker concentrations *versus* time relationships.

In general, peripheral drug distribution can be lumped into identifiable volumes and clearances: a fast nondistributive peripheral pathway (V_{ND-F} and Cl_{ND-F}); a slow nondistributive peripheral pathway (V_{ND-S} and Cl_{ND-S}); rapidly (fast) equilibrating tissues (V_{T-F} and Cl_{T-F}); and slowly equilibrating tissues (V_{T-S} and Cl_{T-S}). The fast and slow nondistributive peripheral pathways (delay elements) represent intravascular circuits in the ICG and inulin models; the only identifiable nondistributive peripheral pathway in the antipyrine model, determined by the recirculation peak, represents blood flow that quickly returns the lipophilic marker to the central circulation after minimal apparent tissue distribution (*i.e.*, a pharmacokinetic shunt).[10,14] In the inulin and antipyrine models, the parallel rapidly and slowly equilibrating tissues are the fast and slow compartments of traditional three-compartment pharmacokinetic models, respectively; therefore, the central circulation and nondistributive peripheral pathway(s) are detailed representations of the ideal central volume of the three-compartment model.[21] Because of the direct correspondence between the recirculatory model and three-compartment models, Cl_E was modeled from the arterial (sampling) compartment to enable comparison of these results with previous ones.

AUC

The AUC was determined for both the first-pass fit ($AUC_{first\text{-}pass}$, calculated for the sum of two parallel Erlang functions) and for the full recirculatory model.[12] The AUCs for the full model were calculated for the interval 0–3 min ($AUC_{0\text{-}3\ min}$) because most intravenous drugs used in the practice of anesthesia (*e.g.*, hypnotics and muscle relaxants) have demonstrable onset within this time. $AUC_{0\text{-}3\ min}$ is the sum of $AUC_{first\text{-}pass}$, which is determined by CO (*i.e.*, $AUC_{first\text{-}pass}$ = dose/CO), and the AUC resulting from marker recirculation (AUC_{recirc}). To resolve the factors influencing $AUC_{0\text{-}3\ min}$, both $AUC_{first\text{-}pass}$ and AUC_{recirc} were determined.

Statistical Analysis

The effects of treatment as well as the order of treatment on observed pharmacokinetic parameters were assessed using a general linear model analysis of variance for a Latin square experimental design (NCSS 6.0.2 Statistical System for Windows; Number Cruncher Statistical Systems, Kaysville, UT). *Post hoc* analysis was conducted using Scheffé multiple comparison test. The relationship of the pharmacokinetic parameters to CO and end-tidal isoflurane concentration was sought using standard least squares linear regression and the Spearman rank order correlation, respectively, (SigmaStat SPSS, Chicago, IL) using the Bonferroni correction of the criterion for rejection of the null hypothesis. The criterion for rejection of the null hypothesis was $P < 0.05$.

Table 1. Subject Characteristics and Global Pharmacokinetic Parameters*

							ICG		Inulin†		Antipyrine†	
End-tidal Isoflurane	Weight (kg)	Hct (%)	HR‡ (BPM)	MAP‡§‖ (mmHg)	CO‡§‖ (l/min)	SVR‡‖ (dyn · s · cm^{-5})	V_{ss} (l/kg)	Cl_E (ml · min^{-1} · kg^{-1})	V_{ss} (l/kg)	Cl_E§‖ (ml · min^{-1} · kg^{-1})	V_{ss} (l/kg)	Cl_E§‖ (ml · min^{-1} · kg^{-1})
0%	28.4	37.3	80	102	4.55	2190	0.080	9.93	0.24	3.40	0.76	6.61
(Awake)	(5.9)	(3.4)	(22)	(8)	(1.13)	(490)	(0.009)	(2.60)	(0.05)	(0.28)	(0.11)	(1.27)
1.7%	28.4	33.3#	111	78#	3.64	1727	0.075	8.22#	0.25	2.84	0.68	2.49#
	(5.9)	(4.0)	(11)	(6)	(0.36)	(103)	(0.007)	(1.59)	(0.03)	(0.25)	(0.08)	(0.60)
2.6%	28.4	30.4#**	105	54#**	2.81#	1582	0.076	7.70#	0.21	2.51	0.68	2.25#
	(5.9)	(2.1)	(2)	(7)	(0.24)	(134)	(0.004)	(1.68)	(0.02)	(0.33)	(0.19)	(0.46)
3.5%	28.4	34.8#††	103	46#**	1.95#**	1820	0.078	7.93#	0.24	1.16#**††	0.76	2.08#
	(5.9)	(0.5)	(8)	(3)	(0.18)	(56)	(0.004)	(2.52)	(0.03)	(0.95)	(0.09)	(0.30)

Data are mean (SD).

* V_{ss}, the sum of all compartmental volumes, is the volume of distribution at steady-state; Cl_E is the elimination clearance.

† Inulin and antipyrine V_{ss} and Cl_E are presented on the basis of plasma rather than blood concentrations.

‡ SVR = MAP × 80/CO, assuming CVP = 0. HR, MAP, CO and SVR are the average of values determined every 10–15 min from time t = 0 to t = 60 min.

§ Correlated with end-tidal isoflurane concentration ($P < 0.05$) as determined by Spearman rank-order correlation.

‖ Correlated with dye (ICG) dilution cardiac output ($P < 0.05$) as determined by least-squares linear regression.

Different from Awake control ($P < 0.05$), as determined by Scheffe multiple comparison test.

** Different from 1.7% isoflurane ($P < 0.05$), as determined by Scheffe multiple comparison test.

†† Different from 2.6% isoflurane ($P < 0.05$), as determined by Scheffe multiple comparison test.

ICG = indocyanine green; Hct = hematocrit; HR = heart rate; MAP = mean arterial pressure; CO = thermal dilution cardiac output; SVR = systemic vascular resistance.

Results

There were large and isoflurane dose-related decreases in blood pressure and CO, whereas heart rate increased slightly and systemic vascular resistance decreased slightly, but not significantly, during isoflurane anesthesia (table 1). The thermal dilution COs (averaged over t = 0 to t = 60 min; table 1) and dye (ICG) dilution COs (determined once at t = 0; table 2) were similar, indicating our sampling schedule and identification of first-pass data were appropriate. The hematocrit also de-

Table 2. Pharmacokinetic Parameters for Recirculatory Indocyanine Green Kinetic Model

	Volumes (l)*				Clearances (l/min)†			
End-tidal Isoflurane	V_C	V_{ND-F}	V_{ND-S}	V_{ss}	Cl_{ND-F}‡§	Cl_{ND-S}‡§	Cl_E	ΣCl‡
0%	0.78	0.16	1.30	2.24	2.16	2.95	0.27	5.38
(Awake)	(0.12)	(0.10)	(0.35)	(0.40)	(0.90)	(0.58)	(0.04)	(1.30)
1.7%	0.59	0.10	1.42	2.11	0.94‖	2.10‖	0.23‖	3.27‖
	(0.15)	(0.03)	(0.34)	(0.45)	(0.25)	(0.38)	(0.02)	(0.21)
2.6%	0.66	0.14	1.37	2.17	0.87‖	1.26‖#	0.21‖	2.35‖
	(0.18)	(0.07)	(0.30)	(0.55)	(0.20)	(0.07)	(0.03)	(0.19)
3.5%	0.63	0.12	1.43	2.18	0.56‖	0.88‖#	0.22‖	1.66‖#
	(0.12)	(0.03)	(0.23)	(0.37)	(0.17)	(0.04)	(0.05)	(0.11)

Data are mean (SD).

* The volumes (V) of the central (C), rapidly equilibrating (fast) nondistributive (ND-F), and slowly equilibrating nondistributive (ND-S) intravascular circuits and the volume of distribution at steady-state (V_{ss}), which equals the sum of all volumes.

† The clearances (Cl) of the rapidly (fast) equilibrating nondistributive (ND-F) and slowly equilibrating nondistributive (ND-S) intravascular circuits, elimination clearance (E), and the sum of all clearances (ΣCl), which equals the ICG (dye dilution) cardiac output determined at the moment of marker injection.

‡ Correlated with end-tidal isoflurane concentration ($P < 0.05$), as determined by Spearman rank-order correlation.

§ Correlated with cardiac output ($P < 0.05$), as determined by least-squares linear regression.

‖ Different from Awake control ($P < 0.05$), as determined by Scheffe multiple comparison test.

Different from 1.7% isoflurane ($P < 0.05$), as determined by Scheffe multiple comparison test.

ICG = indocyanine green.

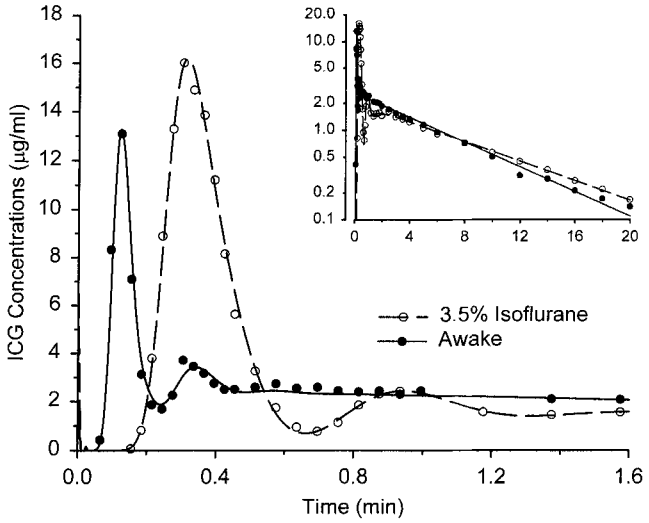

Fig. 2. Arterial blood indocyanine green (ICG) concentration histories for the first 2.0 min (illustrating the first- and second-pass peaks) and for 20 min, or to the limit of detection, (*inset*) after right atrial injection in one dog when it was awake (closed symbols) and when it was anesthetized with 3.5% isoflurane (open symbols). The symbols represent measured ICG concentrations, and the lines represent concentrations predicted by the models.

creased slightly but significantly with increasing isoflurane concentrations (table 1).

Global Model Parameters

The blood ICG, inulin, and antipyrine concentration *versus* time relationships were well characterized by the models from the moment of injection (time t = 0; figs. 2–4). The one-sample runs test did not identify systematic deviations of the observed data from the calculated values. As described below, our recirculatory model of physiologic marker disposition was able to describe the effect of isoflurane anesthesia on CO and its distribution (the ICG model; table 2) and the effect of reduced and redistributed CO on inulin (table 3) and antipyrine (table 4) disposition. The total volumes of distribution (V_{SS}) of ICG, inulin, and antipyrine were unaffected by isoflurane anesthesia (tables 1–4), but their Cl_Es were significantly decreased by isoflurane, as reflected in the decreased slopes of their terminal marker concentration *versus* time relationships (tables 1–4 and insets of figs. 2–4).

ICG

Isoflurane anesthesia had no effect on the volumes of the central and peripheral circulations described by ICG disposition; nearly 30% of the blood volume was in the central circuit (V_C), less than 10% was in the fast nondistributive circuit ($V_{ND\text{-}F}$), and approximately 60% was in the slow nondistributive circuit ($V_{ND\text{-}S}$) (fig. 1 and table 2). Isoflurane produced a progressive and dose-related decrease in flow through the central circuit (dye-dilution CO), from a 36% reduction at 1.7% isoflurane to a 68% reduction at 3.5% isoflurane. Both the fast nondistributive intercompartmental clearance ($Cl_{ND\text{-}F}$) and the slow nondistributive intercompartmental clearance ($Cl_{ND\text{-}S}$) of ICG were significantly correlated with end-tidal isoflurane concentration and were significantly different from the baseline value at all end-tidal isoflurane concentrations. Flows through each circuit decreased directly in proportion to the decrease in CO ($Cl_{ND\text{-}F}$ = 0.45 CO − 0.30, R^2 = 0.86; $Cl_{ND\text{-}S}$ = 0.54 CO + 0.10, R^2 = 0.90), hence the fractions of the CO not represented by Cl_E (*i.e.*, 87–95% of CO) flowing through $Cl_{ND\text{-}F}$ and through $Cl_{ND\text{-}S}$ were approximately 40% and 60%, respectively, under all experimental conditions.

Inulin

The volumes of the recirculatory inulin pharmacokinetic model were also largely unaffected by isoflurane anesthesia; approximately 20% of the volume of inulin was in the central and peripheral nondistributive circuits (V_C, $V_{ND\text{-}F}$, and $V_{ND\text{-}S}$), whereas nearly 30% of the volume was the rapidly equilibrating (fast) tissue ($V_{T\text{-}F}$), and the balance was the slowly equilibrating tissue ($V_{T\text{-}S}$) (table

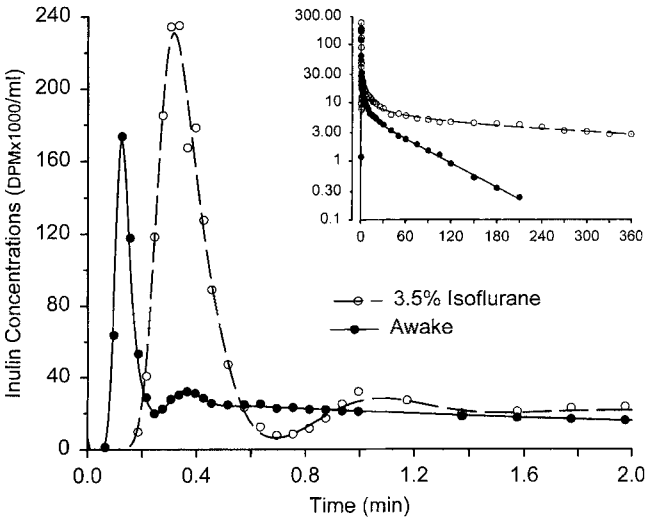

Fig. 3. Arterial blood inulin concentration histories for the first 2.0 min (illustrating the first- and second-pass peaks) and to the limit of detection (*inset*) after right atrial injection in one dog when it was awake (closed symbols) and when it was anesthetized with 3.5% isoflurane (open symbols). The symbols represent measured inulin concentrations, and the lines represent concentrations predicted by the models.

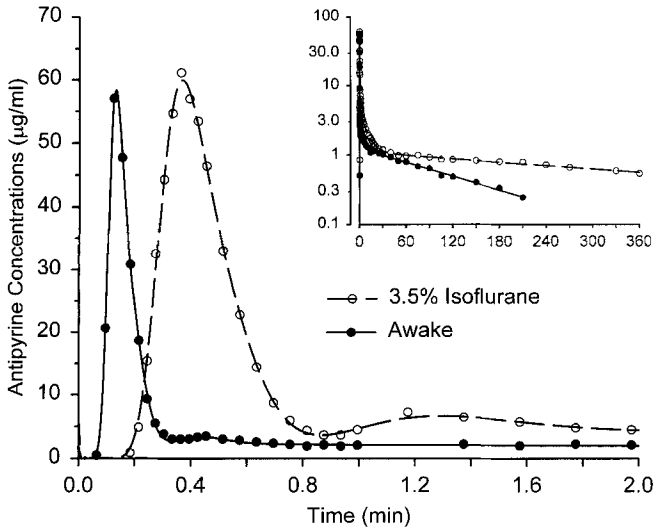

Fig. 4. Arterial blood antipyrine concentration histories for the first 2.0 min (illustrating the first- and second-pass peaks) and for 360 min, or to the limit of detection (*inset*), after right atrial injection in one dog when it was awake (closed symbols) and when it was anesthetized with 3.5% isoflurane (open symbols). The symbols represent measured antipyrine concentrations, and the lines represent concentrations predicted by the models.

3). All inulin clearances, except that to the fast nondistributive circuit ($Cl_{ND\text{-}F}$), were correlated with end-tidal isoflurane concentrations; $Cl_{ND\text{-}F}$ decreased significantly at 1.7% isoflurane and remained essentially unchanged at higher isoflurane concentrations. Both $Cl_{ND\text{-}F}$ and $Cl_{ND\text{-}S}$ were correlated with CO ($Cl_{ND\text{-}F}$ = 0.59 CO − 0.86, R^2 = 0.75; $Cl_{ND\text{-}S}$ = 0.25 CO + 0.67, R^2 = 0.53). Approximately 75% of CO was nondistributive in the inulin models in the dogs under all experimental conditions because the transcapillary distribution of inulin is limited by free water diffusion, not blood flow. Neither the fast nor the slow distributive (intercompartmental, tissue) clearance ($Cl_{T\text{-}F}$ and $Cl_{T\text{-}S}$) of inulin was correlated with CO, but both decreased significantly at 2.6% and 3.5% isoflurane. Inulin Cl_E (glomerular filtration rate) was significantly less than the baseline value only at 3.5% isoflurane.

Antipyrine

Although the total volume of distribution did not change, the antipyrine peripheral distribution volumes were affected by isoflurane anesthesia (table 4). As the rapidly equilibrating (fast) tissue volume ($V_{T\text{-}F}$) decreased in an isoflurane dose-dependent and CO-related manner ($V_{T\text{-}F}$ = 1.37 CO + 0.05, R^2 = 0.91), the slowly equilibrating tissue volume ($V_{T\text{-}S}$) increased in such a way that together they always accounted for 95% of the antipyrine distribution volume. The central (V_C), pulmonary tissue ($V_{T\text{-}P}$), and the peripheral nondistributive volumes (V_{ND}) were unaffected by isoflurane anesthesia.

Despite the profound effect of isoflurane on CO, antipyrine nondistributive clearance (Cl_{ND}) did not change,

Table 3. Pharmacokinetic Parameters for Recirculatory Inulin Pharmacokinetics

End-tidal Isoflurane	Volumes (l)*						Clearances (l/min)†					
	V_C	$V_{ND\text{-}F}$	$V_{ND\text{-}S}$	$V_{T\text{-}F}$	$V_{T\text{-}S}$	V_{SS}	$Cl_{ND\text{-}F}$§	$Cl_{ND\text{-}S}$‡§	$Cl_{T\text{-}F}$‡	$Cl_{T\text{-}S}$‡	Cl_E‡	ΣCl‡
0%	0.78	0.22	1.04	3.07	5.60	10.72	2.29	1.92	0.85	0.17	0.15	5.38
(Awake)	(0.12)	(0.19)	(0.33)	(1.21)	(1.59)	(3.11)	(1.59)	(0.14)	(0.33)	(0.04)	(0.03)	(1.30)
1.7%	0.59	0.08	1.24	3.25	5.24	10.39	0.57‖	1.90	0.55	0.13‖	0.12	3.27‖
	(0.15)	(0.05)	(0.25)	(0.93)	(0.71)	(1.97)	(0.30)	(0.31)	(0.09)	(0.04)	(0.01)	(0.21)
2.6%	0.66	0.14	1.30	2.56#	3.99	8.65	0.71	1.21‖#	0.26‖	0.07‖#	0.10	2.35‖
	(0.18)	(0.08)	(0.65)	(0.75)	(0.46)	(2.02)	(0.22)	(0.07)	(0.11)	(0.02)	(0.01)	(0.19)
3.5%	0.63	0.13	1.17	2.57#	5.76	10.25	0.46‖	0.78‖#**	0.29‖	0.08‖#	0.05‖#	1.66‖#
	(0.11)	(0.01)	(0.39)	(0.96)	(0.81)	(1.12)	(0.17)	(0.17)	(0.13)	(0.04)	(0.04)	(0.11)

Data are mean (SD).

* The volumes (V) of the central (C), rapidly equilibrating (fast) nondistributive (ND-F), and slowly equilibrating nondistributive (ND-S) circuits and the rapidly equilibrating (fast) (T-F) and slowly equilibrating (T-S) tissues, and the volume of distribution at steady-state (V_{SS}), which equals the sum of all volumes.

† The clearances (Cl) of the rapidly equilibrating (fast) nondistributive (ND-F) and slowly equilibrating nondistributive (ND-S) circuits and the rapidly equilibrating (fast) (T-F) and slowly equilibrating (T-S) tissues, elimination clearance (E), and the sum of all clearances (ΣCl), which equals the ICG (dye dilution) cardiac output determined at the moment of marker injection.

‡ Correlated with end-tidal isoflurane concentration ($P < 0.05$), as determined by Spearman rank-order correlation.

§ Correlated with cardiac output ($P < 0.05$), as determined by least-squares linear regression.

‖ Different from Awake control ($P < 0.05$), as determined by Scheffe multiple comparison test.

Different from 1.7% isoflurane ($P < 0.05$), as determined by Scheffe multiple comparison test.

** Different from 2.6% isoflurane ($P < 0.05$), as determined by Scheffe multiple comparison test.

Table 4. Pharmacokinetic Parameters for Recirculatory Antipyrine Pharmacokinetics

End-tidal Isoflurane	Volumes (l)*						Clearances (l/min)†				
	V_C	V_{T-P}	V_{ND}	V_{T-F}‡§	V_{T-S}	V_{SS}	Cl_{ND}	Cl_{T-F}‡§	Cl_{T-S}‡	Cl_E‡§	ΣCl:
0%	0.78	0.09	0.14	7.79	12.78	21.58	0.54	3.87	0.79	0.187	5.38
(Awake)	(0.12)	(0.03)	(0.12)	(1.68)	(4.57)	(3.58)	(0.26)	(1.29)	(0.32)	(0.035)	(1.30)
1.7%	0.59	0.10	0.15	3.80‖	16.06‖	20.69	0.71	1.77‖	0.72	0.074‖	3.27‖
	(0.15)	(0.03)	(0.04)	(0.76)	(3.44)	(4.14)	(0.13)	(0.18)	(0.25)	(0.014)	(0.21)
2.6%	0.66	0.11	0.17	3.14‖	15.50	19.59	0.65	1.24‖	0.39‖#	0.065‖	2.35‖
	(0.18)	(0.05)	(0.12)	(0.33)	(5.36)	(5.92)	(0.22)	(0.24)	(0.08)	(0.015)	(0.19)
3.5%	0.63	0.13‖#	0.18	2.77‖	16.92‖	20.63	0.49	0.76‖	0.35‖#	0.057‖	1.66‖
	(0.11)	(0.03)	(0.02)	(0.39)	(3.00)	(3.49)	(0.16)	(0.03)	(0.09)	(0.012)	(0.11)

Data are mean (SD).

* The volumes (V) of the central (described by ICG and inulin) circuit (C), pulmonary tissue (the difference between the antipyrine central circuit volume and th described by ICG and inulin) (T-P), nondistributive (ND) circuit, and the rapidly equilibrating (fast) (T-F) and slowly equilibrating (T-S) tissues, and the volume distribution at steady-state (V_{SS}), which equals the sum of all volumes.

† The clearances (Cl) of the nondistributive (ND) circuit and the rapidly equilibrating (fast) (T-F) and slowly equilibrating (T-S) tissues, elimination clearance (E), ar the sum of all clearances (ΣCl), which equals the ICG (dye dilution) cardiac output determined at the moment of marker injection.

‡ Correlated with end-tidal isoflurane concentration ($P < 0.05$), as determined by Spearman rank-order correlation.

§ Correlated with cardiac output ($P < 0.05$), as determined by least-squares linear regression.

‖ Different from Awake control ($P < 0.05$), as determined by Scheffe multiple comparison test.

Different from 1.7% isoflurane ($P < 0.05$), as determined by Scheffe multiple comparison test.

ICG = indocyanine green.

as a result of which the fraction of CO represented by Cl_{ND} increased from approximately 10% of CO in awake animals to nearly 30% of the reduced CO in 3.5% isoflurane anesthetized animals (table 4). Antipyrine tissue distribution clearances (Cl_{T-F} and Cl_{T-S}) and Cl_E decreased in an isoflurane dose-dependent manner. As a result of the CO-related decrease in Cl_{T-F} (Cl_{T-F} = 0.85 CO − 0.78, R^2 = 0.96), the fraction of CO repr sented by Cl_{T-F} decreased from 71% in awake animals t 46% in 3.5% isoflurane-anesthetized animals. Cl_{T-S} wa approximately 20% of CO, and Cl_E was nearly 3% of C in all experimental conditions. Thus, the fraction of C represented by Cl_{N-D} increased with isoflurane anesth sia at the expense of Cl_{T-F}.

Table 5. Total Areas Under the Blood Concentrations of the Physiologic Markers *versus* Time Relationships ($AUC_{0-3\ min}$) and Those without Contribution from First-pass (AUC_{recirc}) for the First 3 min after Right Atrial Injection of ICG, Inulin, and Antipyrine

End-tidal Isoflurane	ICG (μg-min/ml)		Inulin (DPM-min/ml × 10^4)		Antipyrine (μg-min/ml)	
	$AUC_{0-3\ min}$	AUC_{recirc}	$AUC_{0-3\ min}$*†	AUC_{recirc}	$AUC_{0-3\ min}$*†	AUC_{recirc}*-
0%	5.88	4.95	5.49	4.25	9.83	5.06
(Awake)	(0.72)	(0.81)	(0.85)	(0.96)	(1.02)	(0.52)
1.7%	6.58	5.09	6.56‡	4.57	16.33‡	8.92‡
	(1.02)	(0.97)	(1.00)	(0.92)	(2.47)	(2.20)
2.6%	6.72	4.65	7.90‡§	5.13	21.67‡§	11.41‡
	(1.10)	(0.97)	(1.29)	(1.18)	(9.66)	(6.83)
3.5%	6.87‡	3.92	8.66‡§	4.73	26.17‡§‖	11.65‡
	(0.87)	(0.97)	(1.04)	(1.15)	(2.60)	(2.98)

Data are mean (SD).

* Correlated with end-tidal isoflurane concentration ($P < 0.05$), as determined by Spearman rank-order correlation.

† Correlated with cardiac output ($P < 0.05$), as determined by least-squares linear regression.

‡ Different from Awake control ($P < 0.05$), as determined by Scheffe multiple comparison test.

§ Different from 1.7% isoflurane ($P < 0.05$), as determined by Scheffe multiple comparison test.

‖ Different from 2.6% isoflurane ($P < 0.05$), as determined by Scheffe multiple comparison test.

ICG = indocyanine green.

AUC

Indocyanine green $AUC_{0\text{-}3\ min}$ was significantly increased only at 3.5% isoflurane (fig. 2 and table 5) due to an increase in $AUC_{first\text{-}pass}$ (*i.e.*, the CO-determined value) since there were no isoflurane-induced changes in ICG AUC_{recirc}. Inulin and antipyrine $AUC_{0\text{-}3\ min}$s increased in an isoflurane dose-dependent manner to more than 1.6 and 2.5 times awake values, respectively, at 3.5% isoflurane (figs. 3 and 4, table 5). The inulin and antipyrine $AUC_{0\text{-}3\ min}$s also increased with decreasing CO ($AUC_{0\text{-}3\ min,\ inulin} \times 10^3 = -7.45\ CO + 95.07$, $R^2 = 0.55$; $AUC_{0\text{-}3\ min,\ antipyrine} = -3.81\ CO + 30.55$, $R^2 = 0.82$). Antipyrine AUC_{recirc} more than doubled in an isoflurane dose-dependent and CO-related manner ($AUC_{recirc,\ antipyrine} = -1.62\ CO + 14.37$, $R^2 = 0.60$), but the inulin AUC_{recirc} did not. Thus, during isoflurane anesthesia, antipyrine $AUC_{0\text{-}3\ min}$ increased because of not only the increase in $AUC_{first\text{-}pass}$ secondary to the decreased CO, but also the increased fraction of CO represented by nondistributive blood flow.

Discussion

Our recirculatory pharmacokinetic model[10] accurately describes changes in physiologic marker disposition due to altered CO and regional blood flow distribution caused by potent volatile anesthetics. In a previous publication, we reported the effects of halothane[14] and now describe the effect of isoflurane, which has been reported to cause more peripheral vasodilation.[15] In these studies, isoflurane and halothane were used as means to create changes in CO and regional blood flow distribution to allow us to study the effects of these physiologic changes on marker disposition rather than to study the affects of the anesthetics *per se*. In both of these studies, in addition to the inhalation anesthetic in oxygen, each dog initially received methohexital and was mechanically ventilated, each of which may contribute to results different from those achieved with an inhalation anesthetic alone. Nonetheless, although the three different levels of inhaled anesthetics in both of these repeated measures studies were each given with the same anesthetic adjuncts, most of the significant changes observed were correlated with end-tidal anesthetic concentration. Thus, in the present study we determined the impact of isoflurane-induced alterations in CO and its distribution on the disposition of physiologic markers acting as surrogates for various intravenous drugs used in the practice of anesthesia.

The observed isoflurane-induced decrease in mean arterial pressure, CO, and systemic vascular resistance (table 1) are consistent with the cardiovascular effects of isoflurane observed by other investigators,[27-29] as is the decrease in hematocrit.[27]

In the recirculatory pharmacokinetic models, CO can flow through either distributive (*i.e.*, tissue) or nondistributive circuits. ICG $Cl_{ND\text{-}F}$, which represents nonsplanchnic (*e.g.*, muscle) blood flow,[10] and ICG $Cl_{ND\text{-}S}$, which represents the splanchnic blood flow,[10] were consistently approximately 40% and 60% of CO under all experimental conditions. Inulin nondistributive blood flow was always 75% of CO and was nearly evenly divided between $Cl_{ND\text{-}F}$ and $Cl_{ND\text{-}S}$ in awake animals, but during isoflurane anesthesia inulin $Cl_{ND\text{-}F}$ and $Cl_{ND\text{-}S}$ represented approximately 40% and 60% of nondistributive blood flow, respectively. Nondistributive antipyrine clearance (Cl_{ND}) was represented by a single peripheral pathway,[10] the absolute value of which was not affected by isoflurane anesthesia despite the decreasing CO with increasing isoflurane concentration. As a result, the fraction of CO that antipyrine Cl_{ND} represented increased from 10% in the awake animals to 30% in dogs anesthetized with 3.5% isoflurane.

The rapidly equilibrating (fast) inulin and antipyrine tissue volumes ($V_{T\text{-}F}$) represent splanchnic tissues, and the slowly equilibrating tissue volumes ($V_{T\text{-}S}$) represent nonsplanchnic tissues.[30] Although the total antipyrine peripheral tissue volume ($V_{T\text{-}F} + V_{T\text{-}S}$) was not affected by isoflurane anesthesia, the fraction of tissue volume represented by $V_{T\text{-}F}$ decreased from nearly 40% in the awake animals to approximately 20% in isoflurane-anesthetized animals. Total clearance to these tissue volumes ($Cl_{T\text{-}F} + Cl_{T\text{-}S}$) decreased compared with the awake total up to 75% in absolute terms and from 87% of CO in awake animals to 67% of CO in 3.5% isoflurane-anesthetized animals. The fraction of distributive blood flow represented by $Cl_{T\text{-}F}$ decreased from 83% in awake animals to 68% in 3.5% isoflurane-anesthetized animals because the fraction of CO represented by $Cl_{T\text{-}F}$ decreased during anesthesia, whereas that represented by $Cl_{T\text{-}S}$ remained constant. In contrast to antipyrine, the inulin tissue volumes were little affected by isoflurane, and total distributive blood flow for inulin remained a relatively constant 20% of CO, with $Cl_{T\text{-}F}$ representing approximately 80% of that total under all experimental conditions.

Given that some pharmacokinetic heterogeneity exists within single tissue types,[31] the shift in both antipyrine tissue volume and distributive blood flow from the rapidly equilibrating tissues to the slowly equilibrating tis-

sues could be explained by a change in the balance of tissue blood supply that is not apparent in the ICG or inulin models. For example, radioactive microsphere studies revealed an isoflurane dose-dependent decrease in preportal blood flow due to both a decrease in CO and vasodilation, yet total hepatic blood flow was only slightly changed by isoflurane because hepatic arterial blood flow nearly doubled.[27,28,32,33] Similar but more subtle changes might occur in muscle beds due to a change in the balance of their dual circulations.[34]

The marker elimination clearances (Cl_E) were all decreased by isoflurane anesthesia (tables 1–4). ICG Cl_E was only modestly affected by isoflurane (tables 1 and 2), but antipyrine Cl_E was dramatically affected by isoflurane, presumably as a result of inhibition of the hepatic mixed function oxidase system responsible for its metabolism.[35,36] Inulin Cl_E was similarly decreased by isoflurane due to decreased glomerular filtration rate.[37] The $AUC_{0-\infty}$ of a complete drug concentration history can increase significantly as a result of a decrease in the Cl_E of the drug ($AUC_{0-\infty}$ = dose/Cl_E). This Cl_E-dependent increase in AUC is readily apparent in the curves in the insets of figures 2–4. However, changes in Cl_E of these low Cl_E markers cannot explain the increase in the marker AUCs in the first minutes after marker administration, long before Cl_E becomes the major determinant of the drug concentration *versus* time relationships (figs. 2–4).

The progressive decreases in CO with increasing isoflurane concentrations are associated with the expected increases in $AUC_{first\text{-}pass}$ ($AUC_{first\text{-}pass}$ = dose/CO) for each marker (figs. 2–4). In isoflurane-anesthetized animals, ICG and inulin $AUC_{0\text{-}3\ min}$s were greater than those in awake animals (tables 2–4), but these differences were due to the large differences in $AUC_{first\text{-}pass}$s (table 5). In contrast, the increase in antipyrine $AUC_{0\text{-}3\ min}$ during isoflurane anesthesia was due to both a decreased CO ($AUC_{first\text{-}pass}$) and an increased amount of marker returning to the central circulation (AUC_{recirc}; table 5). Increased return of antipyrine to the central circulation during isoflurane anesthesia was therefore due to maintenance of the apparent flow of blood not involved in marker distribution to the tissues (*i.e.*, Cl_{ND}), despite an isoflurane-induced decrease in CO, at the expense of decreased $Cl_{T\text{-}F}$ (table 4). Thus, isoflurane-induced changes in CO and its distribution alters the balance of antipyrine nondistributive and distributive blood flows to various tissues that are not proportional to changes in CO. Similar changes in inulin AUC are not observed because, despite an isoflurane-induced alteration in the balance of inulin $Cl_{ND\text{-}F}$ and $Cl_{ND\text{-}S}$, the proportion of CO represented by all nondistributive flow in the inulin model was unaffected by isoflurane anesthesia.

Although the isoflurane-induced increase in the fraction of CO represented by Cl_{ND} in the antipyrine model can be due to the opening of arteriovenous anastomoses or an increase in significant diffusion barriers, it is most likely due to opening of arteriovenous anastomoses. Increased arteriovenous shunting is consistent with observed shunt rates of 9-μm radiolabeled microspheres through arteriovenous anastomoses in control and isoflurane-anesthetized dogs.[38] Their control shunt rate of 8.9% is consistent with the 9.6% of CO that antipyrine Cl_{ND} represented in our awake dogs, whereas the shunt rates of 19.9% and 17.4% in dogs anesthetized with 1% and 2% isoflurane, respectively, are consistent with the 21.6% of CO that antipyrine Cl_{ND} represented in our dogs when they were anesthetized with 1.7% isoflurane. Isoflurane dose-related increases in the shunting of microspheres have been observed in other studies.[28]

The effects of isoflurane on marker distribution is quite different from that observed in dogs under different levels of halothane anesthesia[14] and in mildly and moderately hypovolemic dogs.[12] Antipyrine AUC was increased in the first minutes after marker administration in all three paradigms of decreased CO and its altered distribution. In contrast to isoflurane, which reduced CO but maintained antipyrine Cl_{ND} and therefore increased it as a percentage of CO, halothane actually increased antipyrine Cl_{ND} both absolutely and as a percentage of CO. Total antipyrine distribution clearance (*i.e.*, $Cl_{T\text{-}F}$ + $Cl_{T\text{-}S}$) during all levels of isoflurane anesthesia was always at least twice Cl_{ND}, whereas at the highest halothane concentrations (*i.e.*, at 2.0% halothane, equivalent minimum alveolar concentration to 3.5% isoflurane), Cl_{ND} equaled total distribution clearance. Moderate hypovolemia produced a decrease in CO similar to that of 1.7% isoflurane and, like isoflurane, had no effect on the absolute value of antipyrine Cl_{ND}, but the antipyrine AUC did not increase as much during moderate hypovolemia as it did during isoflurane anesthesia because $Cl_{T\text{-}F}$ was a higher fraction of CO during hypovolemia and $V_{T\text{-}F}$ was unaffected by hypovolemia.

The increased arterial antipyrine concentrations (fig. 4) and the consequent increase in $AUC_{0\text{-}3\ min}$ up to 2.5 times awake values during isoflurane anesthesia (table 5) is the result of both a decreased CO ($AUC_{first\text{-}pass}$) and increased fraction of CO represented by nondistributive blood flow (AUC_{recirc}; table 4). The increased antipyrine

AUC in the first minutes after rapid intravenous administration simulates the expected increased drug exposure of the sites of action of lipophilic drugs with a rapid onset of effect, for which antipyrine is a pharmacokinetic surrogate.[10,21,39] This increased drug exposure would be expected to result in a more profound and prolonged effect.[11] Because the majority of CO in the recirculatory inulin model is nondistributive and the balance between distributive and nondistributive clearance is unaffected by isoflurane anesthesia (table 3), the increase in early arterial inulin concentrations (fig. 3) and the consequent increase in $AUC_{0\text{-}3\ min}$ (table 5) during isoflurane anesthesia is less pronounced than that of antipyrine. Therefore, the onset and duration of effect of the hydrophilic drugs for which inulin is a surrogate (*e.g.*, the relatively slow onset neuromuscular blockers)[10] will be less affected than that of more rapid-onset lipophilic drugs.

These data provide further evidence, along with those from similar studies in dogs under different levels of halothane anesthesia[14] and in volume-loaded as well as mildly and moderately hypovolemic dogs,[12] that not only CO but also its peripheral distribution affect early physiologic marker concentration history after rapid intravenous administration.[1] These studies have also demonstrated that changes in antipyrine distribution are not proportional to changes in CO. Furthermore, the relative impact of CO and regional blood flow changes on early marker disposition vary, depending on the characteristics of the marker being studied and the physiologic circumstances of the subject. Alteration in CO and its distribution are likely to provide the pharmacokinetic bases of interindividual differences in response to drugs with a rapid onset of effect, such as thiopental.[1,4]

References

1. Krejcie TC, Avram MJ: What determines anesthetic induction dose? It's the front-end kinetics, Doctor! (Editorial). Anesth Analg 1999; 89:541-4

2. Price HL: A dynamic concept of the distribution of thiopental in the human body. ANESTHESIOLOGY 1960; 21:40-5

3. Henthorn TK, Krejcie TC, Avram MJ: The relationship between alfentanil distribution kinetics and cardiac output. Clin Pharmacol Ther 1992; 52:190-6

4. Avram MJ, Sanghvi R, Henthorn TK, Krejcie TC, Shanks CA, Fragen RJ, Howard KA, Kaczynski DK: Determinants of thiopental induction dose requirements. Anesth Analg 1993; 76:10-7

5. Wada DR, Bjorkman S, Ebling WF, Harashima H, Harapat S, Stanski DR: Computer simulation of the effects of alterations in blood flows and body composition on thiopental pharmacokinetics in humans. ANESTHESIOLOGY 1997; 87:884-99

6. Ludbrook GL, Upton RN: A physiological model of induction of anaesthesia with propofol in sheep. 2. Model analysis and implications for dose requirements. Br J Anaesth 1997; 79:505-13

7. Upton RN, Ludbrook GL, Grant C, Martinez AM: Cardiac output is a determinant of the initial concentrations of propofol after short-infusion administration. Anesth Analg 1999; 89:545-52

8. Egan TD, Kuramkote S, Gong G, Zhang J, McJames SW, Bailey PL: Fentanyl pharmacokinetics in hemorrhagic shock: A porcine model. ANESTHESIOLOGY 1999; 91:156-66

9. Henthorn TK, Avram MJ, Frederiksen MC, Atkinson AJ Jr: Heterogeneity of interstitial fluid space demonstrated by simultaneous kinetic analysis of the distribution and elimination of inulin and gallamine. J Pharmacol Exp Ther 1982; 222:389-94

10. Krejcie TC, Henthorn TK, Niemann CU, Klein C, Gupta DK, Gentry WB, Shanks CA, Avram MJ: Recirculatory pharmacokinetic models of markers of blood, extracellular fluid and total body water administered concomitantly. J Pharmacol Exp Ther 1996; 278: 1050-7

11. Powis G: Anticancer drug pharmacodynamics. Cancer Chemother Pharmacol 1985; 14:177-83

12. Krejcie TC, Henthorn TK, Gentry WB, Niemann CU, Enders-Klein C, Shanks CA, Avram MJ: Modifications of blood volume alter the disposition of markers of blood volume, extracellular fluid, and total body water. J Pharmacol Exp Ther 1999; 291:1308-16

13. Riggs DS: The Mathematical Approach to Physiological Problems: A Critical Primer. Cambridge, MA, The M.I.T. Press, 1963

14. Avram MJ, Krejcie TC, Niemann CU, Klein C, Gentry WB, Shanks CA, Henthorn TK: The effect of halothane on the recirculatory pharmacokinetics of physiologic markers. ANESTHESIOLOGY 1997; 87:1381-93

15. Eger EI: Isoflurane: A review. ANESTHESIOLOGY 1981; 55:559-76

16. Garner D, Laks MM: New implanted chronic catheter device for determining blood pressure and cardiac output in conscious dogs. Am J Physiol 1985; 249:H681-4

17. Eger EI: Anesthetic Uptake and Action. Baltimore, Williams and Wilkins, 1974

18. Atlee JL III, Brownlee SW, Burstrom RE: Conscious-state comparisons of the effects of inhalation anesthetics on specialized atrioventricular conduction times in dogs. ANESTHESIOLOGY 1986; 64:703-10

19. Grasela DM, Rocci ML Jr, Vlasses PH: Experimental impact of assay-dependent differences in plasma indocyanine green concentration determinations. J Pharmacokinet Biopharm 1987; 15:601-13

20. Bowsher DJ, Krejcie TC, Avram MJ, Chow MJ, del Greco F, Atkinson AJ Jr.: Reduction in slow intercompartmental clearance of urea during dialysis. J Lab Clin Med 1985; 105:489-97

21. Krejcie TC, Henthorn TK, Shanks CA, Avram MJ: A recirculatory pharmacokinetic model describing the circulatory mixing, tissue distribution and elimination of antipyrine in dogs. J Pharmacol Exp Ther 1994; 269:609-16

22. Krejcie TC, Jacquez JA, Avram MJ, Niemann CU, Shanks CA, Henthorn TK: Use of parallel Erlang density functions to analyze first-pass pulmonary uptake of multiple indicators in dogs. J Pharmacokinet Biopharm 1996; 24:569-88

23. Jacquez JA: Compartmental Analysis in Biology and Medicine, 3rd Edition. Ann Arbor, BioMedware, 1996

24. Krejcie TC, Avram MJ, Gentry WB, Niemann CU, Janowski MP, Henthorn TK: A recirculatory model of the pulmonary uptake and pharmacokinetics of lidocaine based on analysis of arterial and mixed venous data from dogs. J Pharmacokinet Biopharm 1997; 25:69-90

25. Berman M, Shahn E, Weiss MJ: The routine fitting of kinetic data to models: A mathematical formalism for digital computers. Biophysical J 1962; 2:275–87

26. Siegel S: Nonparametric Statistics for the Behavioral Sciences. New York, McGraw-Hill, 1956

27. Lundeen G, Manohar M, Parks C: Systemic distribution of blood flow in swine while awake and during 1.0 and 1.5 MAC isoflurane anesthesia with or without 50% nitrous oxide. Anesth Analg 1983; 62:499–512

28. Gelman S, Fowler KC, Smith LR: Regional blood flow during isoflurane and halothane anesthesia. Anesth Analg 1984; 63:557–65

29. Pagel PS, Kampine JP, Schmeling WT, Warltier DC: Comparisonof the systemic and coronary hemodynamic actions of desflurane, isoflurane, halothane, and enflurane in the chronically instrumented dog. ANESTHESIOLOGY 1991; 74:539–51

30. Sedek GS, Ruo TI, Frederiksen MC, Shih S-R, Atkinson AJ Jr: Splanchnic tissues are a major part of the rapid distribution spaces of inulin, urea and theophylline. J Pharmacol Exp Ther 1989; 251:1026–31

31. Crone C: Permeability of single capillaries compared with results from whole-organ studies. Acta Physiol Scand Suppl 1979; 463: 75–80

32. Gelman S, Fowler KC, Smith LR: Liver circulation and function during isoflurane and halothane anesthesia. ANESTHESIOLOGY 1984; 61: 726–30

33. Hartman JC, Pagel PS, Proctor LT, Kampine JP, Schmeling WT, Warltier DC: Influence of desflurane, isoflurane and halothane on regional tissue perfusion in dogs. Can J Anaesth 1992; 39:877–87

34. Renkin EM: Effects of blood flow on diffusion kinetics in isolated perfused hindlegs of cats: A double circulation hypothesis. Am J Physiol 1955; 183:125–36

35. Rahman MM, Fujii K, Kawamoto M, Yuge O: Contrasting effect of isoflurane on drug metabolism: Decreased type I and increased type II substrate metabolism in guinea pig liver microsomes. J Appl Toxicol 1996; 16:331–7

36. Wood M, Wood AJJ: Contrasting effects of halothane, isoflurane, and enflurane on in vivo drug metabolism in the rat. Anesth Analg 1984; 63:709–14

37. Mazze RI, Cousins MJ, Barr GA: Renal effects and metabolism of isoflurane in man. ANESTHESIOLOGY 1974; 40:536–42

38. Yano H, Takaori M: The microcirculation during enflurane and isoflurane anaesthesia in dogs. Can J Anaesth 1994; 41:149–55

39. Renkin EM: Capillary permeability to lipid-soluble molecules. Am J Physiol 1952; 168:538–45